

# Higher Order Integral Nested Sliding Mode Control of Internal Combustion Engine

Marco Meza-Aguilar<sup>1</sup>, Juan Diego Sánchez-Torres<sup>1</sup>, Antonio Navarrete-Guzmán<sup>1</sup>, Jorge Rivera<sup>2</sup>,  
and Alexander G. Loukianov<sup>1</sup>

**Abstract**— In this paper, a controller for internal combustion engine is presented. This scheme is based on the combination of high order sliding mode, integral sliding mode and globally linearizing strategies. That technique is used to find a control law such that output is related linearly to the input, i.e. to find a suitable equation eliminating the non-linearity between output and input. The integral sliding mode control is used to guarantee the robustness of the closed-loop system, and the high order sliding mode control is applied to track the reference signal, to reject perturbations and to estimate a certain unknown value of the system by means of the equivalent control method.

## I. INTRODUCTION

Since, the automotive industry is constantly pursuing to satisfy the end user demand of fuel efficient along with free running of the vehicle, almost every modern car is equipped with on board diagnostics softwares in their electronic control units (ECUs) to control and monitor the engine operations.

The engine speed control problem has been considered in several publications [1]–[4]. Usually, these controllers are based on mean value engine models (MVEMs) [5] due to the fact that these models can describe the behavior of spark ignition (SI) engines [6], [7]. The MVEMs models describe the time development of the most important measurable engine variables on time scales a little larger than an engine cycle [8], [9].

The sliding mode (SM) control approach has been widely used by control engineers for the regulation of dynamic systems. The attractiveness of this control technique is due to its robustness property to matched perturbations [10]. The SM techniques are based on the idea of the sliding manifold, that is an integral manifold with finite reaching time [11]. The integral SM control [12]–[14] has been proposed with the aim to force the system trajectories to start at initial time in the sliding manifold, eliminating in that way the reaching phase and ensuring robustness at the same time. These controllers have been shown high performance and easy implementation as shown in [15]–[18]. However, the basic approach guarantees robustness in

\*This project was supported by the National Council on Science and Technology (CONACYT), México (under grant, 129591).

<sup>1</sup> Marco Meza-Aguilar, Juan Diego Sánchez-Torres, Antonio Navarrete-Guzmán, and Alexander G. Loukianov are with the Department of Electrical Engineering, CINVESTAV-IPN Guadalajara, Av. del Bosque 1145 Col. El Bajío CP 45019, México, e-mail: [ameza, dsánchez, anavarret, louk]@gdl.cinvestav.mx

<sup>2</sup>Jorge Rivera is with Department of Electronics, CUCEI, Guadalajara University, Blvd. Marcelino García Barragán 1421, C.P. 44430, Guadalajara, Jalisco, México, e-mail: jorge.rivera@cucei.udg.mx

presence of the matched disturbances only [19]. To deal with the disturbances affecting the motion on the sliding manifold, that is unmatched disturbances, several methods have been considered. A common and effective approach is the design of sliding manifolds which includes integral actions as in [20]–[22]

As an alternative to the mentioned methods, the integral nested SM algorithms (IN-SM) [23], [24], are based on the application of nested SM control [25] combined with the integral SM control [12]–[14] to nonlinear systems presented in the nonlinear block controllable form [26], [27]. This approach was proposed with the idea to design sliding manifold which includes integral SM terms. In this way, the motion on the sliding manifold has the characteristics of the integral SM controllers, rejecting or attenuating the unmatched disturbances with the nested sliding mode philosophy. The nested SM approach consists in introducing smooth functions that approximate the sing function in the SM dynamics. The approximation function is the sigmoid one. The smoothness of this function allows to continue with the block control design procedure. This proposal allows to design a well defined manifold, however, with reduced robustness and tracking performance. To overcome this major drawback of the IN-SM it was proposed the integral nested higher-order sliding modes (IN-HOSM) algorithms [28], [29] as an extension of IN-SM ones. Using quasi-continuous SM (QC-SM) algorithms [30] instead of sigmoid functions, leads to a nested integral structure but with exact disturbance rejection. It is worth to highlight that the QC-SM algorithms can be designed to be differentiable for each block by selecting a suitable SM order, as it was shown in similar techniques [31], [32].

This work aims to design a robust controller for the internal combustion engine with unknown parameters using the (IN-HOSM) algorithms [28], [29]

The paper is organized as follows: Section II provides the considered model of the MVEM. Section III describes the proposed controllers, including a detailed stability analysis of the designed closed-loop system. Simulation results are presented in Section IV. Finally, in Section V the conclusions are given.

## II. MEAN VALUE ENGINE MODELS

In this section the Mean Value Engine Model (MVEM) of Spark Ignition (SI) is presented [33].

### A. The Crank Shaft Speed State Equation

The crank shaft state equation is derived using straight forward energy conservation considerations. Energy is inserted into the crank shaft via the fuel flow. To avoid the modeling of the cooling and exhaust system losses, the thermal efficiency of the engine is inserted as a multiplier of the fuel mass flow. Losses in pumping and friction dissipate rotational energy while some of the energy goes into the load. Physically this is expressed as a conservation law: the rate of a change of the crank shaft rotational kinetic energy is equal to sum of the power available to accelerate the crank shaft and that of the load:

$$\dot{n}_e = -\frac{(P_f + P_p + P_b)}{J_e n_e} + \frac{H_u \eta_i \dot{m}_f}{J_e n_e} \quad (1)$$

where  $n_e$  is the crank shaft speed,  $J_e$  is the moment of inertia in the rotating parts of the engine,  $P_f$ ,  $P_p$  and  $P_b$  are the power lost to the friction, pumping losses and the load, respectively,  $H_u$  is the fuel burn value,  $\eta_i$  is the thermal efficiency, and  $\dot{m}_f$  is the fuel mass flow.

The loss functions  $P_f$  and  $P_p$  form the load input to the engine and can be implemented to match a desired operating scenario. They are usually regressions based on data from engine measurements and can be modeled by the following regressions functions:

$$\begin{aligned} P_f &= 0.0135n_e^3 + 0.2720n_e^2 + 1.6730n_e \\ P_p &= n_e P_m (0.2060n_e - 0.9690). \end{aligned} \quad (2)$$

where  $P_m$  is the pressure in the intake manifold. It has been found convenient to express the load power as the function:

$$P_b = k_b n^3 \quad (3)$$

where  $k_b$  is the loading parameter. It is adjusted in such a way than the engine is loaded to the desired power or torque level at a given operating point.

The thermal efficiency  $\eta_i$  is also a regression and can be modeled by the following polynomial:

$$\eta_i = 0.55(1 - 0.39n_e^{-0.36})(0.82 + 0.58P_m - 0.39P_m^2). \quad (4)$$

### B. Fuelling System

The fluid film flow model describes the dynamics of the fluid flow through the manifold. The fluid flow  $\dot{m}_f$  has two components: fuel vapor flow and fuel film flow, denoted by  $\dot{m}_{fv}$ ,  $\dot{m}_{ff}$ , respectively [33].

$$\begin{aligned} \dot{m}_{ff} &= \frac{1}{\tau_f}(-\dot{m}_{ff}) + X_f \dot{m}_{fi} \\ \dot{m}_{fv} &= (1 - X_f) \dot{m}_{fi} \\ \dot{m}_f &= \dot{m}_{ff} + \dot{m}_{fv} \end{aligned} \quad (5)$$

where  $\dot{m}_{fi}$  is the injected fuel mass flow,  $X_f$  is the fraction of  $\dot{m}_{fi}$  which is deposited on the manifold as fuel film and  $\tau_f$  is the fuel evaporation time constant (0.25s).

### C. Manifold Pressure State Equation

In the derivation of the manifold pressure state equation, the common procedure is to use the conservation of air mass in the intake manifold:

$$\dot{m}_m = \dot{m}_{ai} - \dot{m}_{ao} \quad (6)$$

where  $\dot{m}_m$  is the air mass flow in the intake manifold,  $\dot{m}_{ai}$  and  $\dot{m}_{ao}$  represent mass flow rate in and out of the intake manifold, i.e. through the throttle valve and into the cylinder, respectively.

The pressure in the intake manifold  $P_m$  can be related to the air mass in the manifold  $m_m$  using the ideal gas equation

$$P_m V_m = m_m R T_m \quad (7)$$

where  $R$  is the ideal gas constant,  $T_m$  is the intake manifold temperature and  $V_m$  is the intake manifold volume.

Taking time derivatives of (7) and using (6), the intake manifold pressure equation is obtained of the form

$$\dot{P}_m = \frac{RT_m}{V_m}(\dot{m}_{ai} - \dot{m}_{ao}). \quad (8)$$

The expressions forms of  $\dot{m}_{ai}$  and  $\dot{m}_{ao}$  are described in the following Subsections.

1) Port Air Mass Flow: The air mass flow  $\dot{m}_{ao}$  at the intake port of the engine can be obtained from the speed-density equation [33] as

$$\dot{m}_{ao} = \sqrt{\frac{T_m}{T_a}} \frac{V_d}{120RT_m} (e_v P_m) n_e. \quad (9)$$

On the other hand, the relation between  $P_m$  and the speed  $n_e$  is given by [34]

$$e_v P_m = s_i P_m - y_i \quad (10)$$

where  $T_a$  is the ambient temperature,  $V_d$  is the engine displacement, the manifold pressure slope  $s_i$  is slightly less than 1 and the manifold pressure intercept  $y_i$  is close to 0.10; they are always positive and depend mostly on the crank shaft speed. Moreover, they should not change much over the range operating an engine from one engine to another except for those which are highly tuned. The form of equation (10) has been known phenomenologically at Ford for many years but in [34] this equation has been derived from physical considerations. This means that it can be rapidly applied to many different engines with basically only a knowledge of a few physical constants, and this is the advantage of the derivation above.

Using now (10) the speed-density equation (9) becomes

$$\dot{m}_{ao} = \sqrt{\frac{T_m}{T_a}} \frac{V_d}{120RT_m} (s_i P_m + y_i) n_e. \quad (11)$$

2) Throttle Air Mass Flow: The second important equation is the manifold pressure state equation, which is used to describe the air mass flow past the throttle plate. This part of the model based on the isoentropic flow equation for a converging-diverging nozzle, is given by [33]

$$\dot{m}_{ai} = \dot{m}_{ai1} \frac{P_a}{\sqrt{T_m}} \beta_1(\alpha) \beta_2(P_r) + \dot{m}_{ao} \quad (12)$$

where  $P_a$  is the ambient pressure,  $\dot{m}_{ai1}$  and  $\dot{m}_{ai0}$  are constants,  $\alpha$  is the throttle angle and  $\beta_1(\alpha)$  is the throttle plate angle dependency which can be described by the following function as an approximation to the normalized open area:

$$\beta_1(\alpha) = 1 - \cos(\alpha) - \frac{\alpha_0^2}{2} \quad (13)$$

where  $\alpha_0$  is the fully closed throttle plate angle (radians). The function  $\beta_1(\alpha)$  serves as the function of an area dependent on the discharge coefficient  $\beta_2(P_r)$ , and it is defined by the isentropic flow expression:

$$\beta_2(P_r) = \begin{cases} \frac{1}{\sqrt{1 - \left(\frac{P_r - P_c}{1 - P_c}\right)}} & P_r < P_c \\ \sqrt{1 - \left(\frac{P_r - P_c}{1 - P_c}\right)} & P_c \leq P_r \end{cases} \quad (14)$$

where  $P_r = P_m/P_a$ , and  $P_c = 0.4125$  is the critical pressure (turbulent flow).

#### D. Internal Combustion Engine Model

The MVEMs state system (1-14), using the state variables  $x = [x_1 \ x_2 \ x_3]^T = [\dot{m}_f \ n_e \ P_m]^T$  is presented in the following form:

$$\begin{aligned} \dot{x}_1 &= \frac{1}{\tau_f}(\dot{m}_{fi} - x_1) + (1 - X_f)\dot{m}_{fi} \\ \dot{x}_2 &= -f_2(x_1, x_2) - b_2(x_2)x_3 \\ \dot{x}_3 &= f_3(x_2, x_3) + b_3(x_3)\beta_1(\alpha) \end{aligned} \quad (15)$$

where

$$\begin{aligned} f_2(x_1, x_2) &= \frac{P_f + P_b}{J_e x_2} + \frac{H_u \eta_i x_1}{J_e x_2}, \quad b_2(x_2) = \frac{0.206x_2 - 0.969}{J_e} \\ f_3(x_2, x_3) &= \frac{RT_m}{V_m}[\dot{m}_{ai0} - \sqrt{\frac{T_m}{T_a}} \frac{V_d}{120RT_m}(s_i x_3 + y_i)x_2], \text{ and} \\ b_3(x_3) &= \frac{RT_m}{V_m} \dot{m}_{ai1} \frac{P_a}{\sqrt{T_m}} \beta_2(P_r). \end{aligned}$$

Defining the input vector  $u = (u_1, u_2)^T$  as  $u_1 = \dot{m}_{fi}$  and  $u_2 = \alpha$  and the output vector  $y = (y_1, y_2)^T = h(x)$  with  $y_1 = \lambda(x)$  and  $y_2 = x_2$ , where  $\lambda(x)$  is the value of air-to-fuel ratio, the system (15) can be written in a controller canonical form:

$$\begin{aligned} \dot{x} &= f(x) + G(x)\tilde{u} \\ y &= h(x) \end{aligned} \quad (16)$$

where

$$\begin{aligned} f(x) &= \begin{bmatrix} -x_1 \\ -f_2(x_1, x_2) - b_2(x_2)x_3 \\ f_3(x_2, x_3) \end{bmatrix} \\ G(x) &= \begin{bmatrix} 1 & 0 \\ 0 & 0 \\ 0 & b_3(x_3) \end{bmatrix} \\ \tilde{u} &= \begin{bmatrix} \tilde{u}_1 \\ \tilde{u}_2 \end{bmatrix} = \begin{bmatrix} \frac{1}{\tau_f}u_1 + (1 - X_f)\dot{u}_1 \\ (1 - \cos(u_2) - \frac{\alpha_0^2}{2}) \end{bmatrix} \end{aligned} \quad (17)$$

### III. CONTROL DESIGN

There are two control objectives: the first is to force the engine speed  $n_e$  to track some desired reference  $n_{er}$ , and the second one is that the value of air-to-fuel ratio  $\lambda$  must reach the unity that achieves a stoichiometric value of 14.67.

#### A. Control of Air-to-Fuel Ratio

In this subsection, to design a sliding manifold the input-output feedback linearization technique [35] is used. The normalized air-to-fuel ratio is expressed by

$$\lambda = \frac{\dot{m}_{ai}}{14.67\dot{m}_f}. \quad (18)$$

Now, define the output tracking error as

$$e_1 = \lambda - r_1 \quad (19)$$

where  $r_1$  is the reference signal for  $\lambda$ . Then the error dynamics is derived of form

$$\dot{e}_1 = f_0(x) + b_0(x)\tilde{u}_1 + \Delta_1(t) \quad (20)$$

where  $f_0(x) = L_\lambda f(x)$ ,  $b_0(x) = L_\lambda G(x)$  are Lie derivatives, and  $\Delta_1(t) = \dot{r}_1$  is considered as a unknown disturbance term, since it is not easy to measure. It is reasonably assumed that  $L_\lambda G(x) \neq 0$  in some admissible domain. Then the control law is proposed of the following form:

$$\tilde{u}_1 = \frac{u_{sm} - L_\lambda f(x)}{L_\lambda G(x)} \quad (21)$$

with  $u_{sm}$  as the generalized super-twisting algorithm [36]

$$\begin{aligned} u_{sm} &= -k_{11}[|e_1|^{1/2}\text{sign}(e_1) + \mu|e_1|^{3/2}\text{sign}(e_1)] + u_{sm1} \\ u_{sm1} &= -k_{12}[1/2\text{sign}(e_1) + 2\mu e_1 + 3/2\mu^2|e_1|^2\text{sign}(e_1)] \end{aligned} \quad (22)$$

where  $e_1$  is the sliding surface,  $\mu$ ,  $k_{11}$  and  $k_{12}$  are the control gains.

Substitute to the original control (17) into (21), yields to

$$\begin{aligned} \dot{u}_1 &= \frac{1}{1 - X_f} \left[ \tilde{u}_1 - \frac{u_1}{\tau_f} \right] \\ &= \frac{1}{1 - X_f} \left[ \frac{u_{sm} - L_\lambda f(x)}{L_\lambda G(x)} - \frac{u_1}{(1 - X_f)\tau_f} \right] \end{aligned} \quad (23)$$

#### B. Engine Speed Control Design

The control law to engine speed  $n_e$  is define as follows. Define the engine speed tracking error as

$$e_2 = n_e - n_{er} = x_2 - x_{2r} \quad (24)$$

where  $n_{er}$  is a reference signal. From (15) and (24), the error dynamics can be derived of the form

$$\dot{e}_2 = -f_{21}(x_2) - b_2(x_2)x_3 - \dot{x}_{2r} + \Delta_2(x) \quad (25)$$

where  $f_{21} = \frac{P_f + P_b}{J_e x_2}$ . The term  $\Delta_2(x)$

$$\Delta_2(x) = \frac{H_u \eta_i x_1}{J_e x_2} \quad (26)$$

is considered in (25) as an unknown disturbance term since it contains the unknown thermal efficiency  $\eta_i$ .

To stabilize the dynamics for  $e_2$  in (25), the variable  $x_3$  can be considered as a virtual control. Then the desired value for  $x_3$ , i.e.  $x_{3des}$  is determined as

$$x_{3des} = x_{3des}^0 + x_{3des}^1 + x_{3des}^2 \quad (27)$$

where  $x_{3des}^1$  will be designed to reject the disturbance  $\Delta_2(x)$  in finite time by using the integral sliding mode technique [14] in combination with quasicontinuous SM control [30]. The term  $x_{3des}^2$  will be designed to cancel the known derivative  $\dot{x}_{2r}$ . The term  $x_{3des}^0$  will be chosen such that  $e_2(t)$  exponentially converges to zero.

Having  $x_{3des}$  (25), the error  $e_3$  is defined as

$$e_3 = x_3 - x_{3des} \quad (28)$$

and (25) can be rewritten of the form

$$\begin{aligned} \dot{e}_2 &= -f_{21}(x_2) - b_2(x_2)x_{3des}^0 - b_2(x_2)x_{3des}^1 \\ &\quad - b_2(x_2)x_{3des}^2 + \Delta_2(x) - \dot{x}_{2r}. \end{aligned} \quad (29)$$

Choose  $x_{3des}^2$  as

$$x_{3des}^2 = -b_2^{-1}(x_2)\dot{x}_{2r}. \quad (30)$$

To design  $x_{3des}^1$ , we define the sliding variable  $\sigma_2$  as

$$\sigma_2 = e_2 - z_2 \quad (31)$$

where  $z_2$  is an integral variable to be defined below. From (25), (30) and (31), the dynamics for  $\sigma_2$  are given by

$$\begin{aligned} \dot{\sigma}_2 &= -f_{21}(x_2) - b_2(x_2)x_{3des}^0 - b_2(x_2)x_{3des}^1 \\ &\quad + \Delta_2(x) + \dot{z}_2 \end{aligned} \quad (32)$$

where  $\dot{z}_2$  is selected of the form

$$\dot{z}_2 = f_{21}(x_2) + b_2(x_2)x_{3des}^0 \quad (33)$$

with  $z_2(0) = e_2(0)$  in order to fulfill the requirement  $\sigma_2(0) = 0$ . With this selection of  $\dot{z}_2$ , system (32) reduces to

$$\dot{\sigma}_2 = -b_2(x_2)x_{3des}^1 + \Delta_2(x) \quad (34)$$

To enforce sliding motion on the manifold  $\sigma_2 = 0$  despite of the disturbance  $\Delta_2(x)$ , the term  $x_{3des}^1$  in (34) is chosen as

$$x_{3des}^1 = b_2^{-1}(x_2)\zeta \quad (35)$$

with  $\zeta$  as the solution of [30]

$$\dot{\zeta} = -\alpha \frac{\dot{\sigma}_2 + \beta|\sigma_2|^{1/2}\text{sign}(\sigma_2)}{|\dot{\sigma}_2| + \beta|\sigma_2|^{1/2}} \quad (36)$$

where  $\alpha > 0$  and  $\beta > 0$ .

When the SM motion on the manifold  $\sigma_2 = 0$  is reached, the equivalent value  $b_2\{x_{3des}^1\}_{eq}$  as a solution of  $\dot{\sigma}_2 = 0$  (32) is calculated of the form

$$b_2\{x_{3des}^1\}_{eq} = \Delta_2(x) \quad (37)$$

This shows that the disturbance  $\Delta_2(x)$  is rejected by the equivalent virtual control  $\{x_{3des}^1\}_{eq}$  [10]. Having  $\{x_{3des}^1\}_{eq} = b_2^{-1}\zeta$  (34) and using (37) and then (26) the estimated value  $\hat{\eta}_i$  of thermal efficiency  $\eta_i$  can be obtained as

$$\hat{\eta}_i = \frac{\zeta x_2 J_e}{H_u x_1}. \quad (38)$$

As result, the dynamics (29) are reduced on  $\sigma_2 = 0$  to

$$\dot{e}_2 = -f_{21} - b_2(x_2)x_{3des}^0. \quad (39)$$

Thus, to stabilize (39) the desired dynamics  $k_2 e_2$  are introduced by means of

$$x_{3des}^0 = b_2^{-1}(x_2)[k_2 e_2 - f_{21}(x_2)] \quad (40)$$

with  $k_2 > 0$ . Having (40) the dynamics  $\dot{z}_2$  (33) reduce to

$$\dot{z}_2 = k_2 e_2 \quad (41)$$

From (28) it follows that

$$\dot{e}_3 = f_3(x_2, x_3) + b_3(x_3)\tilde{u}_2 - \dot{x}_{3des} \quad (42)$$

where pseudo control  $\tilde{u}_2$  is proposed as follows:

$$\tilde{u}_2 = b_3^{-1}(x_3)(\dot{x}_{3des} - f_3(x_2, x_3) + u_{st}) \quad (43)$$

where the derivative  $\dot{x}_{3des}$  is obtained by a sliding mode exact robust differentiator [37], and to enforce sliding motion on the manifold  $e_3 = 0$  (28), the control  $u_{st}$  in (43) is chosen using super twisting algorithm [37]:

$$\begin{aligned} u_{st} &= u_{st1} + u_{st2} \\ u_{st1} &= -k_{21}|e_3|^{1/2}\text{sign}(e_3) \\ \dot{u}_{st2} &= -k_{22}\text{sign}(e_3) \end{aligned} \quad (44)$$

with the control gains  $k_{21} > 0$  and  $k_{22} > 0$ .

By using (13) the final expression for the control results as follows:

$$u_2 = \cos^{-1}(1 - \tilde{u}_2 - \frac{\alpha_0^2}{2}) \quad (45)$$

### C. Closed-loop system stability

Using the nonsingular transformation (19), (24), (35), (30) and (40)

$$\begin{aligned} e_1 &= \lambda - r \\ e_2 &= x_2 - x_{2des} \\ e_3 &= x_3 - b_{12}^{-1}(k_2 e_2 - f_{12}(e_2) + \zeta - \dot{x}_{2des}) \\ \sigma_2 &= e_2 + z_2 \end{aligned} \quad (46)$$

with the integral variable  $z_2$  and  $\zeta$  defined by (41), and (36) respectively; the extended closed loop system (20), (25) and (42) is presented as

$$\begin{cases} \dot{e}_1 &= -k_{11}[|e_1|^{1/2}\text{sign}(e_1) + \mu|e_1|^{3/2}\text{sign}(e_1)] \\ &\quad + u_{12} + \Delta_1(t) \\ \dot{u}_{21} &= -k_{12}[1/2\text{sign}(e_1) + 2\mu e_1 + 3/2\mu^2|e_1|^2\text{sign}(e_1)] \end{cases} \quad (47)$$

$$\begin{cases} \dot{e}_2 &= -k_2 e_2 - \zeta + b_{12} e_3 + \Delta_2(x) \end{cases} \quad (48)$$

$$\begin{cases} \dot{\sigma}_2 &= -\zeta + b_{12} e_3 + \Delta_2(x) \\ \dot{\zeta} &= -\alpha \frac{\dot{\sigma}_2 + \beta|\sigma_2|^{1/2}\text{sign}(\sigma_2)}{|\dot{\sigma}_2| + \beta|\sigma_2|^{1/2}} \end{cases} \quad (49)$$

$$\begin{cases} \dot{e}_3 &= -k_{21}|e_3|^{1/2}\text{sign}(e_3) + u_{21} \\ \dot{u}_{21} &= -k_{22}\text{sign}(e_3). \end{cases} \quad (50)$$

Considering the disturbances in the closed-loop system (47)-(50) as fulfilling the following conditions:

$$\begin{aligned} |\dot{\Delta}_1(t)| &\leq L_1 \\ |\dot{\Delta}_2(x)| &\leq L_2 \end{aligned} \quad (51)$$

in some admissible region  $\Omega_0$  with  $L_1 > 0$  and  $L_2 > 0$ , the stability of the closed-loop system (47)-(50) is outlined in the stepwise procedure

**(Step A)** Reaching phase of the projection motion (50).

**(Step B)** The SM stability of the projection motion (49).

**(Step C)** The SM motion stability of (48) on the manifold  $e_3 = 0$ .

**(Step D)** Reaching phase of the projection motion (47).

**Step A)** If we select  $k_{21} > 0$  and  $k_{22} > 0$ , the system (50) will be finite time stable [38], i.e. this solution converges to the origin  $e_3 = 0$  in finite time.

**(Step B)** For (49), the motion on the manifold  $e_3 = 0$  is described by

$$\begin{aligned} \dot{\sigma}_2 &= -\zeta + \Delta_2(x) \\ \dot{\zeta} &= -\alpha \frac{\dot{\sigma}_2 + \beta|\sigma_2|^{1/2}\text{sign}(\sigma_2)}{|\dot{\sigma}_2| + \beta|\sigma_2|^{1/2}} \end{aligned} \quad (52)$$

by applying the change of variables  $\psi_1 = \sigma_2$  and  $\psi_2 = \dot{\sigma}_2$ , the system (52) is written as

$$\begin{aligned} \dot{\psi}_1 &= \psi_2 \\ \dot{\psi}_2 &= -\alpha \frac{\dot{\psi}_1 + \beta|\psi_1|^{1/2}\text{sign}(\psi_1)}{|\dot{\psi}_1| + \beta|\psi_1|^{1/2}} + \dot{\Delta}_2(x) \end{aligned} \quad (53)$$

under condition (51), there exist  $\alpha > 0$  and  $\beta > 0$  such that a solution of the system (53) converges to the origin  $(\psi_1, \psi_2) = (\sigma_2, \dot{\sigma}_2) = (0, 0)$  in finite time, inducing a SM motion on  $\sigma_2 = 0$  [30].

**(Step C)** The motion for (48) on the set  $(e_3, \sigma_2) = (0, 0)$  given by

$$\dot{e}_2 = -k_2 e_2 \quad (54)$$

with  $k_2 > 0$  is exponentially stable.

**(Step D)** Using the transformation  $q = u_{12} + \Delta_1(t)$ , the system (47) yields to

$$\begin{aligned} \dot{e}_1 &= -k_{11}[|e_1|^{1/2}\text{sign}(e_1) + \mu|e_1|^{3/2}\text{sign}(e_1)] + q \\ \dot{q} &= -k_{12}[1/2\text{sign}(e_1) + 2\mu e_1 + 3/2\mu^2|e_1|^2\text{sign}(e_1)] \\ &\quad + \dot{\Delta}_1(t) \end{aligned} \quad (55)$$

Under the assumption (51), it follows that if  $k_{11} > 0$  and  $k_{22} > 3L_1 + 4(\frac{L_1}{k_{11}})^2$ , then the equilibrium point  $(e_1, q) = (0, 0)$  finite time despite of the perturbation  $\Delta_1(t)$  [36].

#### IV. SIMULATIONS

In this Section, we verify the performance of the proposed control scheme by means of numerical simulations.

We consider a MVEMs with the following nominal parameters [34]:  $V_d = 1.275$  L,  $R = 0.00287$ ,  $V_m = 0.0017$ ,  $I = 480(2\pi/60)^2$ ,  $H_u = 4300$ ,  $L_{th} = 14.67$ ,  $\lambda = 1.0$ ,  $T_m = 293$ ,  $T_a = 293$ ,  $P_c = 0.4125$ ,  $P_a = 1.013$ ,

$P_r = P_m/P_a$ ,  $\dot{m}_{ai1} = 5.9403$ ,  $\dot{m}_{ai0} = 0$ ,  $si = 0.961$ ,  $yi = -0.07$ . The velocity reference signal starts from 1.5 krpm and it increases to 2 krpm in the first 5 s and then it remains constant for 5 to 9 s, again increases from 2 krpm to 3 krpm of 9 to 18 s, and finally in 4 krpm it remains constant for 18 to 30 s.

In Figure 1 it is shown the output tracking response of  $\lambda$ ; it presents an acceptable performance even in the presence of an perturbation. The response of the engine speed is shown in Figure 2, it has a good behavior even in the value of the thermal efficiency  $\eta_i$  is unknown. This value is estimated by SM, as it is shown in Figure 3. Finally, Figure 4 shows the traking errors  $e_2$  and  $e_3$  responses.

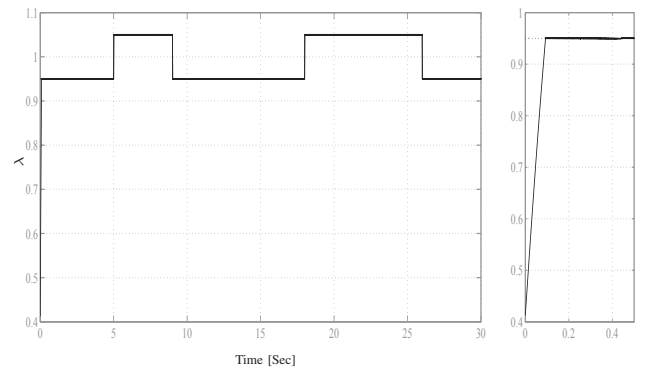


Fig. 1: Value of air-to-fuel ratio  $\lambda$  (solid) and reference  $r_1$  (dashed).

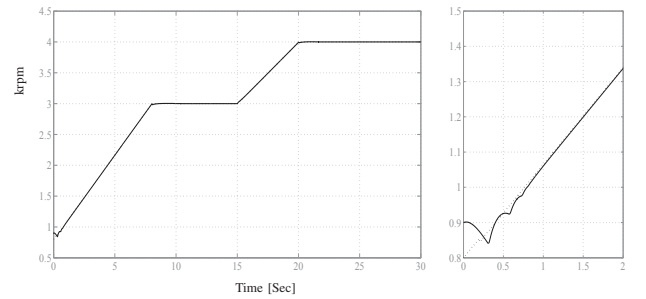


Fig. 2: Velocity engine  $n_e$  (solid) and reference  $n_{er}$  (dashed).

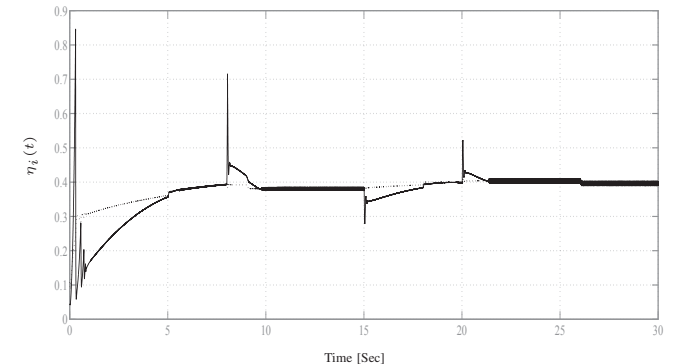


Fig. 3: Unknown function  $\eta_i$  (dashed) and its estimation  $\hat{\eta}_i$  (solid).

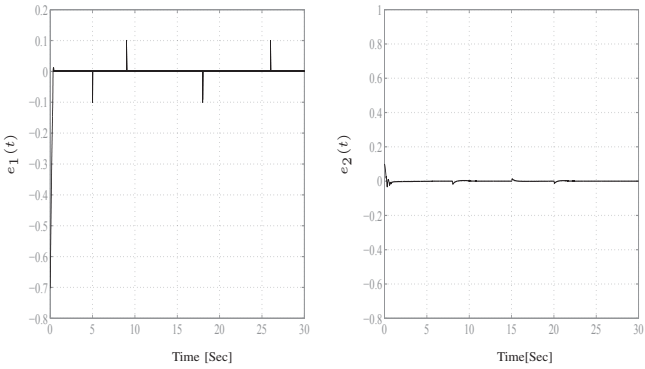


Fig. 4: Tracking errors  $e_1$  and  $e_2$ .

## V. CONCLUSIONS

The proposed control for the internal combustion engine is designed using a combination of integral and high order SM techniques, which ensure finite time stability of the closed-loop system in presence of unmatched engine parameters variations. Simulations results show efficiency of the proposed control scheme.

## REFERENCES

- [1] A. G. Loukianov, S. Dodds, W. Hosny, and J. Vittek, "A robust automotive controller design," in *Control Applications, 1997. Proceedings of the 1997 IEEE International Conference on*, 1997, pp. 806–811.
- [2] J. J. Moskwa and J. Hedrick, "Automotive engine modeling for real time control application," in *American Control Conference*, 1987, pp. 341–346.
- [3] L. Guzzella and C. Onder, *Introduction to Modeling and Control of Internal Combustion Engine Systems*. Springer, 2009.
- [4] Q. Ahmed and A. Bhatti, "Second order sliding mode observer for estimation of si engine volumetric efficiency amp; throttle discharge coefficient," in *Variable Structure Systems (VSS), 2010 11th International Workshop on*, 2010, pp. 307–312.
- [5] E. Hendricks and S. Sorenson, "Mean value si engine model for control studies," in *American Control Conference, 1990*, 1990, pp. 1882–1887.
- [6] E. Hendricks and T. Vesterholm, "The analysis of mean value si engine models," in *SAE Technical Paper*, 1992.
- [7] E. Hendricks and S. Sorenson, "Mean value modelling of spark ignition engines," in *SAE Technical Paper*, no. 900616, 1990.
- [8] E. Hendricks, "Mean value modelling of large turbocharged two-stroke diesel engines," in *SAE Technical Paper*, 1989.
- [9] R. Rajamani, *Vehicle Dynamics and Control*, ser. Mechanical Engineering. Springer, 2012.
- [10] V. I. Utkin, *Sliding Modes in Control and Optimization*. Springer Verlag, 1992.
- [11] S. V. Drakunov and V. I. Utkin, "Sliding mode control in dynamic systems," *International Journal of Control*, vol. 55, pp. 1029–1037, 1992.
- [12] G. P. Matthews and R. A. DeCarlo, "Decentralized tracking for a class of interconnected nonlinear systems using variable structure control," *Automatica*, vol. 24, no. 2, pp. 187 – 193, 1988.
- [13] V. I. Utkin and J. Shi, "Integral sliding mode in systems operating under uncertainty conditions," in *Decision and Control, 1996. Proceedings of the 35th IEEE Conference on*, vol. 4, 1996, pp. 4591–4594 vol.4.
- [14] V. I. Utkin, J. Guldner, and J. Shi, *Sliding Mode Control in Electro-Mechanical Systems, Second Edition (Automation and Control Engineering)*, 2nd ed. CRC Press, 5 2009.
- [15] K. Abidi, J.-X. Xu, and Y. Xinghuo, "On the discrete-time integral sliding-mode control," *Automatic Control, IEEE Transactions on*, vol. 52, no. 4, pp. 709–715, 2007.
- [16] B. Castillo-Toledo, S. Di Gennaro, A. G. Loukianov, and J. Rivera, "Hybrid control of induction motors via sampled closed representations," *Industrial Electronics, IEEE Transactions on*, vol. 55, no. 10, pp. 3758–3771, 2008.
- [17] L. E. González Jiménez, A. Loukianov, and E. Bayro-Corrochano, "Discrete integral sliding mode control in visual object tracking using differential kinematics," in *Progress in Pattern Recognition, Image Analysis, Computer Vision, and Applications*, ser. Lecture Notes in Computer Science, E. Bayro-Corrochano and J.-O. Eklundh, Eds. Springer Berlin Heidelberg, 2009, vol. 5856, pp. 843–850.
- [18] M. Heertjes and R. Verstappen, "Self-tuning in integral sliding mode control with a Levenberg-Marquardt algorithm," *Mechatronics*, no. -, pp. –, 2013, in press.
- [19] B. Drazenovich, "The invariance conditions in variable structure systems," *Automatica*, vol. 5, pp. 287–295, 1969.
- [20] W.-J. Cao and J.-X. Xu, "Nonlinear integral-type sliding surface for both matched and unmatched uncertain systems," *Automatic Control, IEEE Transactions on*, vol. 49, no. 8, pp. 1355–1360, 2004.
- [21] L. Fridman, A. Poznyak, and F. Bejarano, "Decomposition of the min-max multi-model problem via integral sliding mode," *International Journal of Robust and Nonlinear Control*, vol. 15, no. 13, pp. 559–574, 2005.
- [22] M. Rubagotti, A. Estrada, F. Castanos, A. Ferrara, and L. Fridman, "Integral sliding mode control for nonlinear systems with matched and unmatched perturbations," *Automatic Control, IEEE Transactions on*, vol. 56, no. 11, pp. 2699–2704, 2011.
- [23] J. Rivera and A. Loukianov, "Integral nested sliding mode control: Application to the induction motor," in *Variable Structure Systems, 2006. VSS'06. International Workshop on*, 2006, pp. 110–114.
- [24] H. Huerta-Avila, A. Loukianov, and J. Canedo, "Nested integral sliding modes of large scale power system," in *Decision and Control, 2007 46th IEEE Conference on*, 2007, pp. 1993–1998.
- [25] A. Adhami-Mirhosseini and M. J. Yazdanpanah, "Robust tracking of perturbed nonlinear systems by nested sliding mode control," in *Proc. Int. Conf. Control and Automation ICCA '05*, vol. 1, 2005, pp. 44–48.
- [26] A. G. Loukianov, "Nonlinear block control with sliding mode," *Automation and Remote Control*, vol. 59, no. 7, pp. 916–933, 1998.
- [27] —, "Robust block decomposition sliding mode control design," *Mathematical Problems in Engineering*, vol. 8, no. 4-5, pp. 349–365, 2002.
- [28] J. D. Sanchez-Torres, A. Navarrete, and A. G. Loukianov, "Integral high order sliding mode control of a brake system," in *Congreso Nacional de la Asociación de México de Control Automático 2013*, 2013, pp. 1–6.
- [29] G. J. Rubio, J. D. Sanchez-Torres, J. M. Canedo, and A. G. Loukianov, "Integral high order sliding mode control of single-phase induction motor," in *Electrical Engineering, Computing Science and Automatic Control (CCE), 2013 10th International Conference on*, 2013, pp. 1–6.
- [30] A. Levant, "Quasi-continuous high-order sliding-mode controllers," *Automatic Control, IEEE Transactions on*, vol. 50, no. 11, pp. 1812 – 1816, nov. 2005.
- [31] A. Estrada and L. Fridman, "Quasi-continuous HOSM control for systems with unmatched perturbations," *Automatica*, vol. 46, no. 11, pp. 1916 – 1919, 2010.
- [32] —, "Integral hosc semiglobal controller for finite-time exact compensation of unmatched perturbations," *Automatic Control, IEEE Transactions on*, vol. 55, no. 11, pp. 2645–2649, 2010.
- [33] E. Hendricks and J. B. Luther, "Model and observer based control of internal combustion engines," in *Proc. of the 1st Int. Workshop on Modeling Emissions and Control in Automotive Engines (MECA), Salerno, Italy*, 2001, pp. 9–20.
- [34] E. Hendricks, A. Chevalier, M. Jensen, and S. Sorenson, "Modelling of the intake manifold filling dynamics," in *SAE Technical Paper*, 1996.
- [35] A. Isidori, *Nonlinear Control Systems*, ser. Communications and Control Engineering. Springer, 1995, no. v. 1. [Online]. Available: [http://books.google.com.mx/books?id=FPGzHK\\\_\\\_pto4C](http://books.google.com.mx/books?id=FPGzHK\_\_pto4C)
- [36] E. Cruz-Zavala, J. Moreno, and L. Fridman, "Uniform robust exact differentiator," *Automatic Control, IEEE Transactions on*, vol. 56, no. 11, pp. 2727–2733, 2011.
- [37] A. Levant, "Higher-order sliding modes, differentiation and output-feedback control," *International Journal of Control*, vol. 76, no. 9/10, pp. 924–941, 2003, special issue on Sliding-Mode Control.
- [38] J. Moreno and M. Osorio, "Strict lyapunov functions for the super-twisting algorithm," *Automatic Control, IEEE Transactions on*, vol. 57, no. 4, pp. 1035–1040, 2012.